Cure Kinetics of Ring-Opening Metathesis Polymerization of Dicyclopentadiene[*]

M. R. Kessler[1], S. R. White[2]

[1]Department of Theoretical and Applied Mechanics
[2]Department of Aeronautical and Astronautical Engineering
University of Illinois at Urbana-Champaign
Urbana-Champaign, IL, USA

Abstract: The cure kinetics of polydicyclopentadiene (pDCPD) prepared by ring-opening metathesis polymerization with three different concentrations of Grubbs' catalyst was examined using differential scanning calorimetry (DSC). The experimental data were used to test several different phenomenological kinetic models. The data are best modeled with a "model-free" isoconversional method. This analysis reveals that the activation energy increases significantly for degree of cure greater than 60%. Catalyst concentration is shown to have a large effect on the cure kinetics.
Keywords: differential scanning calorimetry (DSC), kinetics (polym.), activation energy, ROMP, dicyclopentadiene.

INTRODUCTION

Polydicyclopentadiene (pDCPD) is generally a highly crosslinked polymer of high toughness formed by a ring-opening metathesis polymerization (ROMP) of its monomer precursor. The polymerization is highly exothermic due to the relief of ring strain energy and can be initiated by transition-metal alkylidene complexes. A recently developed ruthenium-based catalyst (Grubbs' catalyst) shows high metathesis activity while being tolerant of a wide range of functional groups as well as oxygen and water [1].

The polymerization of DCPD with Grubbs' catalyst in reaction injection molding (RIM) and resin transfer molding (RTM) applications results in a polymer with excellent mechanical properties and little chemical shrinkage [2]. Recently, White *et al.* [3] reported on a materials system that incorporates dicyclopentadiene (DCPD) and Grubbs' catalyst into an epoxy matrix to autonomically repair the material when it is damaged. Similarly, Kessler and White [4] used DCPD to repair delamination damage in laminate composites in which the Grubbs' catalyst was embedded in the matrix of the composite material.

In self-healing applications the polymerization kinetics determine the extent to which polymerization can occur for a given time and at a particular temperature and thus, the healing efficiency. In RIM and RTM applications the kinetics influence the thermochemical history of the part, ultimately dictating the processing time and final physical properties. Modeling the cure kinetics of DCPD and Grubbs' catalyst has utility

---

not only in optimizing self-healing materials, but also the processing of RIM/RTM fabricated pDCPD.

In phenomenological modeling of the cure kinetics of thermosetting polymers an internal state variable is defined to which all other properties are related. This state variable is the degree of cure (α) and ranges from zero (uncured) to one (fully cured). Thermal analysis by differential scanning calorimetry (DSC) is the most commonly used experimental technique to determine the cure kinetics of thermosets [5]. For DSC measurements the degree of cure is defined as

$$\alpha(t) = \frac{H(t)}{H_R} \tag{1}$$

where $H(t)$ is the enthalpy of reaction up to time t, and H_R is the total enthalpy of reaction. The DSC provides a continuous history of the heat evolved during polymerization which can then be integrated to yield $H(t)$ and through Eq. (1) the degree of cure history is obtained.

Traditionally, the determination of kinetic parameters from DSC measurements is accomplished using isothermal data [5]. Isothermal measurements do have the advantage of a complete separation between the variables of time and temperature. However, significant advancement of the cure state can take place before the DSC can reach and stabilize at the desired temperature, and at low temperatures the reaction may not proceed to completion. Alternatively, dynamic data allow for a better capture of the kinetics at both the start and end of a reaction and complex reaction mechanisms can be more easily interpreted by comparing measurements at different heating rates.

In this study a phenomenological cure kinetics model is developed from dynamic DSC data of DCPD cured with Grubbs' catalyst over a range of catalyst concentrations. The experimental data were used to test several different phenomenological kinetic models over a range of heating rates from 2-15°C·min^{-1}.

MATERIALS AND METHODS

Materials. DCPD monomer stabilized with 100 – 200 ppm p-tert-butylcatechol was purchased from Acros Organics (Geel, Belgium). As supplied, the monomer is predominantly endo isomer. The monomer was purified by low vacuum distillation to remove any trace impurities. Bis(tricyclohexylphosphine)benzylidine ruthenium (IV) dichloride (Grubbs' catalyst) was purchased from Strem Chemicals (Newburyport, MA) in the form of a fine purple powder. The catalyst was stored and prepared in a glove box with N$_2$ purge to minimize decomposition over time.

The mixing of DCPD with Grubbs' catalyst initiates the ROMP reaction shown in Figure 1. This ROMP reaction can be extremely rapid at room temperature, depending on the catalyst concentration and sample size. The polymerization of DCPD was accomplished using three different catalyst to monomer ratios as shown in Table 1.

Technique. Vials each containing 20 mg, 30 mg, or 40 mg of catalyst and a small Teflon®-coated magnetic stir bar were placed in a water bath at 15°C. To each was added 15 ml of distilled DCPD, also cooled to 15°C, and the solutions were mixed vigorously using the magnetic stirrer for about 30 seconds, by which time the catalyst powder had dissolved and a homogeneous solution was achieved for the three concentrations listed in Table 1. The vials were then immediately placed in liquid

nitrogen to flash-freeze the solution and stored in a –80°C freezer. A typical DSC sample was prepared by removing a small amount of the frozen solution and placing it in an aluminum DSC pan, weighing the sample, and loading it in the DSC chamber at a standby temperature of –5°C. The average and standard deviation in sample size was 9.8 mg and 1.9 mg, respectively.

DSC measurements were performed using a Mettler Toledo DSC821^e connected to a computer equipped with STAR^e v 6.0 evaluation software to manipulate and transfer data. The DSC cell was swept by a constant flow of nitrogen at 80 ml·min^{-1}. The DSC was first calibrated in duplicate for temperature and heat flow accuracy using indium, water, octane, and zinc standards. Tests were performed on the DCPD/catalyst system in dynamic mode at various heating rates over the temperature range from –50 to 250°C. Data obtained from heating rates of 2, 5, 7, 10, and 15°C·min^{-1} were converted to ASCII format and kinetic analysis was performed using Netzsch Thermokinetics program (v. 2001.2), Mathematica (v. 4.1.1), and standard statistical and plotting programs.

CURE KINETIC MODELING

Model-Fitting Method. In kinetic analysis it is generally assumed that the rate of reaction can be described by two separable functions $K(T)$ and $f(\alpha)$ such that

$$\frac{d\alpha}{dt} = K(T) \cdot f(\alpha) \tag{2}$$

where $d\alpha/dt$ is the rate of reaction, $K(T)$ is the temperature dependent rate constant, and $f(\alpha)$ corresponds to the reaction model. The temperature dependence of the reaction rate is commonly described by the Arrhenius equation

$$K(T) = A \cdot \exp\left(\frac{-E}{RT}\right) \tag{3}$$

where R is the universal gas constant, E is the activation energy and A is the pre-exponential factor.

For experiments in which samples are heated at a constant rate, the explicit time dependence in Eq. (2) can be eliminated so that

$$\frac{d\alpha}{dT} = \frac{A}{\beta} \cdot \exp\left(-\frac{E}{RT}\right) \cdot f(\alpha) \tag{4}$$

where $\beta = dT/dt$ is the heating rate.

A multivariate version of the Borchardt and Daniels method [6] is frequently used in the evaluation of dynamic DSC data. In this method the kinetic parameters (A, E) are obtained by a linearizing transformation of Eq. (4) so that

$$\ln\frac{d\alpha/dT}{f(\alpha)} = \ln\left(\frac{A}{\beta}\right) - \frac{E}{RT} \tag{5}$$

This linear equation, which has the form $y = a_0 + a_1 x$ with $x = 1/T$, can be used to determine the optimal fit of the kinetic parameters by multiple linear regression.

"Model-Free" Isoconversional Method. The "model-free" isoconversional method assumes that both the activation energy and the pre-exponential factor are functions of the degree of cure. The activation energy is determined by Friedman's method [7] from the logarithmic form of the rate equation for each heating rate:

$$\ln\left[\beta_i(d\alpha/dT)_{\alpha,i}\right] = \ln\left(A_\alpha f(\alpha)\right) - \frac{E_\alpha}{RT_{\alpha,i}} \tag{6}$$

where the subscript α is the value at a particular degree of cure and i refers to data from a given heating rate experiment. The activation energy at each degree of cure is calculated using linear regression from a plot of $\ln[\beta_i(d\alpha/dT)_{\alpha,i}]$ versus $1/T_{\alpha,i}$ (Friedman plot) across all of the heating rates tested. Similarly, the product of cure dependent pre-exponential factor and the reaction model can be obtained from the y-intercept of the Friedman plot. These parameters can alternately be calculated by an integral isoconversional method described by Flynn and Wall [8] and Ozawa [9].

The isoconversional approach can be used to evaluate both simple and complex chemical reactions. For evaluation of data using this method no kinetic rate expression is assumed *a priori*.

EXPERIMENTAL RESULTS

A typical DSC scan and the corresponding degree of cure is shown in Figure 2. When the scan begins at –50°C the sample is a frozen solid. Near -5°C a broad endothermic peak initiates and extends from –5 to 15°C. This endothermic peak corresponds to the melting of the DCPD. Superimposed on this melting transition is a sharp endothermic peak at 0°C corresponding to the presence of water in the sample, presumably condensation resulting from the flash freezing of the sample in liquid nitrogen immediately after mixing. Analyzing the size of the peak and assuming 2400 J·g⁻¹ for ΔH of water, the total content of water was determined to be less than 0.005% for all samples analyzed. Later tests on samples that were not flash frozen showed no endothermic melting peak at 0°C, but otherwise were identical to those that were flash frozen. To correct for these melting transitions in the evaluation of the degree of cure, a best fit spline connecting the pre- and post-melt regions was constructed (the dashed line in Figure 2) to effectively eliminate the melting phenomenon from the heat flow curves. As a justification, less than 0.5% of cure advancement occurs before the end of the melting region and as such, has little influence on the overall cure kinetics.

The baseline used to determine the total heat released and the degree of cure is also shown in Figure 2. Subsequent dynamic plots are presented having corrected for the melting transition and subtracting the baseline from the heat flow data. The degree of cure is then calculated from the corrected plots.

Figure 3 shows the DSC scans for all of the experimental runs used to create the kinetic models reported herein. As the catalyst concentration increases, the exothermic peak shifts to lower temperatures for a given heating rate. For the lowest concentration tested (Figure 3a), at 2°C·min⁻¹ there was excessive weight loss (over 9%) from evaporation of DCPD, so this case was discarded and only four heating rates were used for model fitting the low concentration data. Table 2 shows the final and initial sample sizes and the total enthalpy of reaction measured for each sample. The average total enthalpy of reaction for all experiments is 461±14.1 J·g⁻¹ and there was no noticeable dependence on heating rate.

MODEL PERFORMANCE

Five different reaction models (Table 3) were used to fit the experimental data by an appropriate multivariable least-squares regression fitting method. The first- and second-order models are the simplest and only require two fitting parameters (E and A). The nth-order reaction model is more general and allows for better fits to the data by letting the order of the reaction be determined empirically. The most complex models investigated require four fitting parameters and including both the nth-order autocatalysis model and the expanded Prout–Tompkins (autocatalytic) model [10,11]. Ng and Manas-Zloczower [11] used the Prout–Tompkins model for a DCPD-based reaction injection molding (RIM) system and found good agreement with experimental results using an adiabatic temperature rise method where the rate of temperature change is related to the rate of reaction through an energy balance for the adiabatic case.

The results of the multiple linear regression analysis for all the models are listed in Table 4. The experimental fits that were obtained are also shown in Figure 4 for the medium catalyst concentration mixture. Based on the LSQ correlation coefficient (see Appendix) the nth-order autocatalytic model gives the best fit to the data over the heating rates investigated. An F-test statistical analysis (see Appendix) confirms this and the results of the analysis are given in Table 5.

In order to determine a model-free estimation for the activation energy, a Friedman plot is first created by using the logarithmic form of the rate equation (Eq. (6)) for all of the heating rates. A Friedman plot for the medium catalyst concentration case is shown in Figure 5. The activation energy and the product of $A*f(\alpha)$ at each degree of cure is calculated by linear regression at a specific value of α. The straight lines in Figure 5 correspond to these linear fits for α values ranging from 0.02 to 0.98.

The complex dependence of the activation energy on the degree of cure can be seen in Figure 6 for all three catalyst concentrations. It is immediately apparent that the activation energy increases significantly for all three concentrations after the degree of cure reaches about 0.6 and especially near the end of cure. The assumption of constant activation energy (as is the case for all of the reaction models listed in Table 4) is reasonable up to this critical degree of cure, but too restrictive for the entire cure range. One interpretation of this behavior is an apparent decrease of molecular mobility as the degree of cure increases above 0.6 and the polymer gels. It is also apparent that the activation energy for all three catalyst concentrations are quite comparable. Finally, the plot of the product of $\ln[A*f(\alpha)]$ appears to vary similarly to the activation energy with degree of cure. This correspondence is due to the isokinetic relationship [7,12] or the kinetic compensation effect [13] which suggests that the value of $\ln A_\alpha$ varies linearly with E_α. Such a relationship has been observed in the curing and decomposition of numerous other polymer systems [14-17].

A fifteenth-order polynomial was used to fit the E and $\ln[A*f(\alpha)]$ data from Figure 6 and together with Eq. (4), predictions for the cure rate at various heating rates were obtained. Figure 7 shows these model-free predictions compared with the experimental data for the medium catalyst concentration case. Excellent agreement is apparent over all of the heating rates investigated.

Model predictions for isothermal curing at 30°C for the medium catalyst concentration case together with the experimental data for a 15 hr isothermal cure are

plotted in Figure 8. During the first hour of curing the model-free prediction fits the experimental data extremely well. The major differences between the various kinetic models are readily apparent at longer times. Particularly, the model-free prediction suggests that the ultimate degree of cure is significantly lower than any of the reaction models because of the increase in activation energy for $\alpha > 0.6$ (see Figure 6). While the isothermal model-free fit deviates from the experimental values for degrees of cure above 0.5 (Figure 8), it does a much better job of predicting the isothermal cure kinetics than any of the model fitting approaches.

Subsequent to the 15 hr isothermal cure at 30°C, these samples were then scanned at 15°C·min^{-1} from –50 to 220°C in the DSC. These scans for all three catalyst concentrations are shown in Figure 9. Also included in Figure 9 is a dynamic scan at 15°C·min^{-1} of a fully cured (low catalyst concentration) sample, which yields a glass transition temperature of 139°C. The glass transition temperatures after isothermal curing for the low, medium, and high catalyst concentration samples are 28.7, 43.7, 48.7, respectively. It is apparent from the results that further polymerization does not occur until after the sample reaches the glass transition temperature. One reason for the deviation between the model-free prediction and the isothermal data for degrees of cure above 0.5 is the difference in curing conditions. Specifically, the dynamic data upon which the model-free fit is based was obtained by curing above the glass transition temperature whereas the isothermal data eventually reaches conditions in which curing occurs below the glass transition. To more accurately model the isothermal case at degrees of cure above 0.5 a model that includes the influence of the cure dependent glass transition temperature should be employed.

Another feature of the medium and high concentration scans in Figure 9 is the presence of an endothermic peak in the T_g region before the larger exothermic curing peak. Similar endothermic peaks attributed to enthalpic relaxation or physical aging are often seen in glassy polymers as a result of slow cooling through the glass transition region or annealing below T_g [18]. The annealing time and temperature has a large affect on the position and magnitude of these annealing peaks. For the medium and high catalyst concentration cases, the end of the annealing peak is superimposed with the beginning of the exothermic curing peak. Thus, the measured glass transition temperature for these cases slightly overestimates the true T_g. The presence of these superimposed annealing peaks also complicates the measurement of the residual heat of reaction for these cases.

The isothermal model-free predictions for all three catalyst concentrations at 30°C is shown in Figure 10. The predictions show a significant difference between the low and the high concentrations for the time necessary to reach a given degree of cure. For example, the degree of cure for the high catalyst concentration is nearly double that of the low catalyst concentration case after 60 minutes at 30°C.

CONCLUSIONS

In this work, several reaction models were used to analyze dynamic DSC data for the cure of DCPD with three different concentrations of Grubbs' catalyst. It was shown that the catalyst concentration has a large effect on the cure kinetics. Of the standard reaction models, the *n*th-order autocatalytic model performed the best. However, the

model-free isoconversional method provided the best fit of the data over the range of healing rates investigated. From the isoconversional method, the activation energy was shown to increase significantly for $\alpha > 0.6$. As a result, the model-free method predicts a lower degree of cure for long periods of time compared with any of the standard reaction models. This behavior was qualitatively verified by isothermal cure experiments at 30°C.

APPENDIX: STATISTICAL EVALUATION

The correlation coefficient (r) is defined as

$$r = \sqrt{1 - \frac{LSQ}{\sum_{S}(\sum_{k} Y_{s,k}^2 - (\sum_{k} Y_{s,k})^2 / N_s)}} \tag{A1}$$

$$LSQ = \sum_{j=1}^{S} \sum_{k=1}^{N_s} (Y_{j,k} - \hat{Y}_{j,k})^2 \tag{A2}$$

where $Y_{j,k}$ is the measured value, $\hat{Y}_{j,k}$ is the regress value, S is the number of scans, and N_S is the number of measured values in a particular scan.

The F-test compares the residual variances of the individual models against one another. It is used to assess whether there is a statistically significant difference between the models with respect to the quality of fit to the experimental data. The model with the lowest correlation coefficient is typically taken as the reference model. The F-test value is then defined as

$$F_{\exp}(f_1, f_2) = \frac{\sum_{j=1}^{S} \sum_{k=1}^{N_s} (Y_{j,k} - \hat{Y}_{j,k}(\text{model}_1))^2 / f_1}{\sum_{j=1}^{S} \sum_{k=1}^{N_s} (Y_{j,k} - \hat{Y}_{j,k}(\text{model}_2))^2 / f_2} \tag{A3}$$

where f_1 is the degree of freedom of model$_1$ and f_2 is the degree of freedom of model$_2$ (the reference model) [19]. $F_{\exp}$ is then compared with the critical value of the F distribution, $F_{\text{crit}}(f_1, f_2)$, for a given confidence level. An $F_{\exp} < F_{\text{crit}}$ indicates no statistical difference while $F_{\exp} > F_{\text{crit}}$ indicates model$_1$ is significantly better suited to characterize the experimental data.

ACKNOWLEDGMENTS

REFERENCES

[1] Schwab, P.; Grubbs, R. H.; Ziller, J. W. J Am Chem Soc 1996, 118, 100-110

[2] Macosko, C. W. RIM, Fundamentals of Reaction Injection Molding 1989, New York.

[3] White, S. R.; Sottos, N. R.; Geubelle, P. H.; Moore, J. S.; Kessler, M. R.; Sriram, S. R.; Brown, E. N.; Viswanathan, S. Nature 2001, 409, 794-797.

[4] Kessler, M. R.; White, S. R. Compos Part A: Appl Sci Manuf 2001, 32(5), 683-699.

[5] Halley, P. J.; Mackay, M. E. Polym Eng Sci 1996, 36(5), 593-608.

[6] Borchardt, H. J.; Daniels, F. J Am Chem Soc 1957, 79, 41-46.

[7] Friedman, H. L. J Polym Sci Part C: Poly Symp 1963, 6, 183.

[8] Flynn, J. H.; Wall, L. A. J Polym Sci Part B: Polym Lett 1966, 4, 323-328.

[9] Ozawa, T. Bull Chem Soc Japan 1965, 38(38), 1881.

[10] Shin, D. D.; Hahn, H. T. Compos Part A: Appl Sci Manuf 2000, 31, 991-999

[11] Ng, H; Manas-Zloczower, I. Polym Eng Sci 1994, 34(11), 921-928.

[12] Vyazovkin, S. Int J Chem Kinet 1996, 28, 95-101.

[13] Pielichowski, K.; Czub, P.; Pielichowski, J. Polymer 2000, 4381-4388.

[14] Cooney, J. D.; Day, M.; Wiles, D. M. J Appl Polym Sci 1984, 29, 911-923.

[15]MacCallum, J. R.; Munro, M. V. Thermochim Acta 1992, 203, 457.

[16] Montserrat, S.; Flaque, C.; Pages, P.; Malek, J. J Appl Polym Sci 1995, 56, 1413-1421.

[17] Montserrat, S.; Andreu, G.; Cortes, P.; Calventus, Y.; Colomer, P.; Hutchinson, J. M.; Malek, J. J Appl Polym Sci 1996, 61, 1663-1974.

[18] McKenna, G. In Comprehensive Polymer Science, Vol. 2, Polymer Properties; Booth, C.; Price, C., Ed.; Oxford, 1989, pp 311-362.

[19] Netzsch Thermokinetics (v. 2001.2), Statistical Evaluation of Results, program help, 2001.

Table 1 Three concentrations of catalyst analyzed.

Designation	g catalyst/ ml DCPD[*]	Catalyst molecules : DCPD molecules[**]
Low	1.33E-3	1:5000
Medium	2.00E-3	1:3750
High	2.67E-3	1:2500

[*]*Density of DCPD is 1.0710 g/cm³*

[**]*MW of DCPD & catalyst is 132.2 & 822.96, respectively*

Table 2 Sample size and measured total enthalpy of reaction.

Concentration	Heating rate	Sample size		Total enthalpy of reaction
		initial	final	
	(°C/min)	(mg)	(mg)	(J/g)
Low	15	9.3	8.9	456.7
	10	10.3	9.8	459.9
	7	8.3	8.1	453.5
	5	7.8	7.4	443.5
Medium	15	9.1	8.9	463.8
	10	6.3	6.1	457.3
	7	7.2	7.1	461.6
	5	11.6	11.3	478.8
	2	12.6	12.3	436.8
High	15	11.2	11.2	472.6
	10	10.8	10.7	485.3
	7	11.9	11.9	474.1
	5	11.1	11.1	467.5
	2	10.3	10.2	442.6

Table 3 Reaction models evaluated.

Reaction model	Model designation	$f(\alpha)$	Parameters
first-order	F1	$(1-\alpha)$	A, E
second-order	F2	$(1-\alpha)^2$	A, E
nth-order	Fn	$(1-\alpha)^n$	A, E, n
nth-order with autocatalysis	Cn	$(1-\alpha)^n(1+K_{cat}\alpha)$	A, E, n, K_{cat}
Prout–Tompkins equation (autocatalytic)	PT	$(1-\alpha)^n\alpha^m$	A, E, n, m

Table 4 Results of multiple linear regression analysis.

Catalyst concentration	Model designation	log[A] (s^{-1})	E (kJ/mol)	n	K$_{cat}$	m	Correlation coefficient
Low	F1	4.961	51.31	-	-	-	0.9822
	F2	8.563	75.69	-	-	-	0.9788
	Fn	6.199	59.65	1.328	-	-	0.9864
	Cn	4.409	48.76	1.616	0.436	-	0.9917
	PT	5.653	55.50	1.335	-	0.093	0.9865
Medium	F1	4.698	46.55	-	-	-	0.9815
	F2	8.083	67.97	-	-	-	0.9921
	Fn	7.019	61.21	1.671	-	-	0.9934
	Cn	5.281	51.10	1.927	0.365	-	0.9965
	PT	5.899	53.27	1.668	-	0.168	0.9942
High	F1	5.240	48.59	-	-	-	0.9757
	F2	8.834	70.86	-	-	-	0.9938
	Fn	8.657	69.76	1.948	-	-	0.9938
	Cn	6.649	58.16	2.192	0.370	-	0.9966
	PT	7.230	60.02	1.923	-	0.176	0.9947

Table 5 F-test statistical analysis of the model fits in Table 4.

Catalyst concentration			F_{exp} *		
	Cn	PT	Fn	F2	F1
Low	1.00	1.69	1.71	2.67	2.20
Medium	1.00	1.72	1.97	2.38	5.41
High	1.00	1.57	1.79	1.80	6.97

*F_{crit}=1.1 for a 95% confidence level
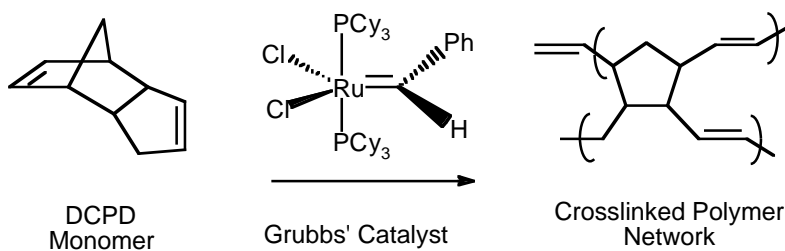
Figure 1. Ring-opening metathesis polymerization (ROMP) of dicyclopentadiene
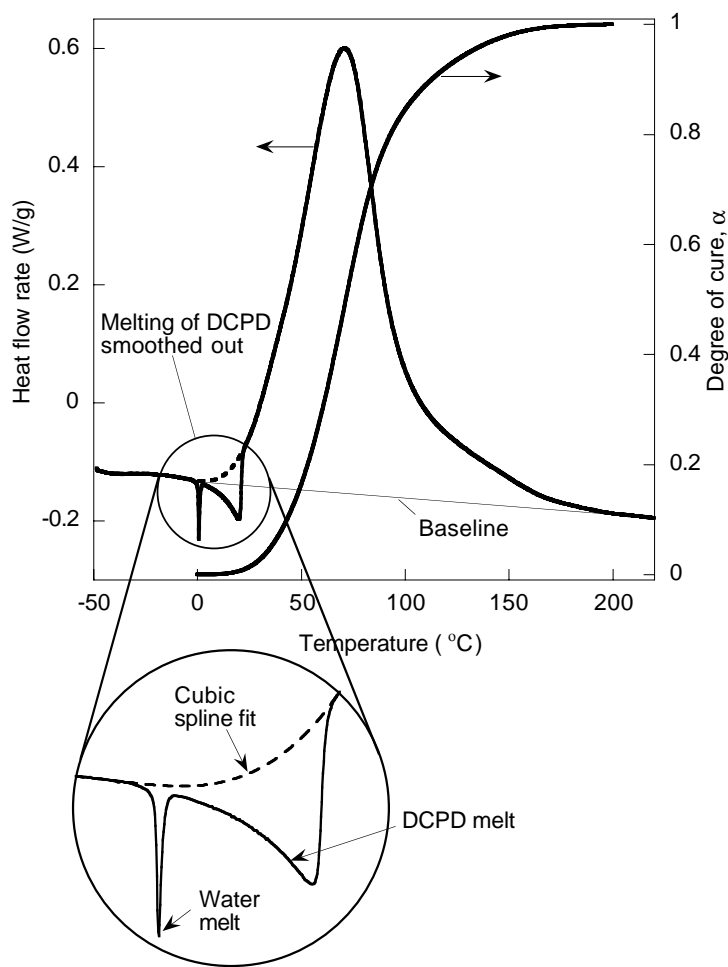(DCPD) with Grubbs' catalyst.

Figure 2. Typical DSC scan (at 5°C/min) and corresponding degree of cure history
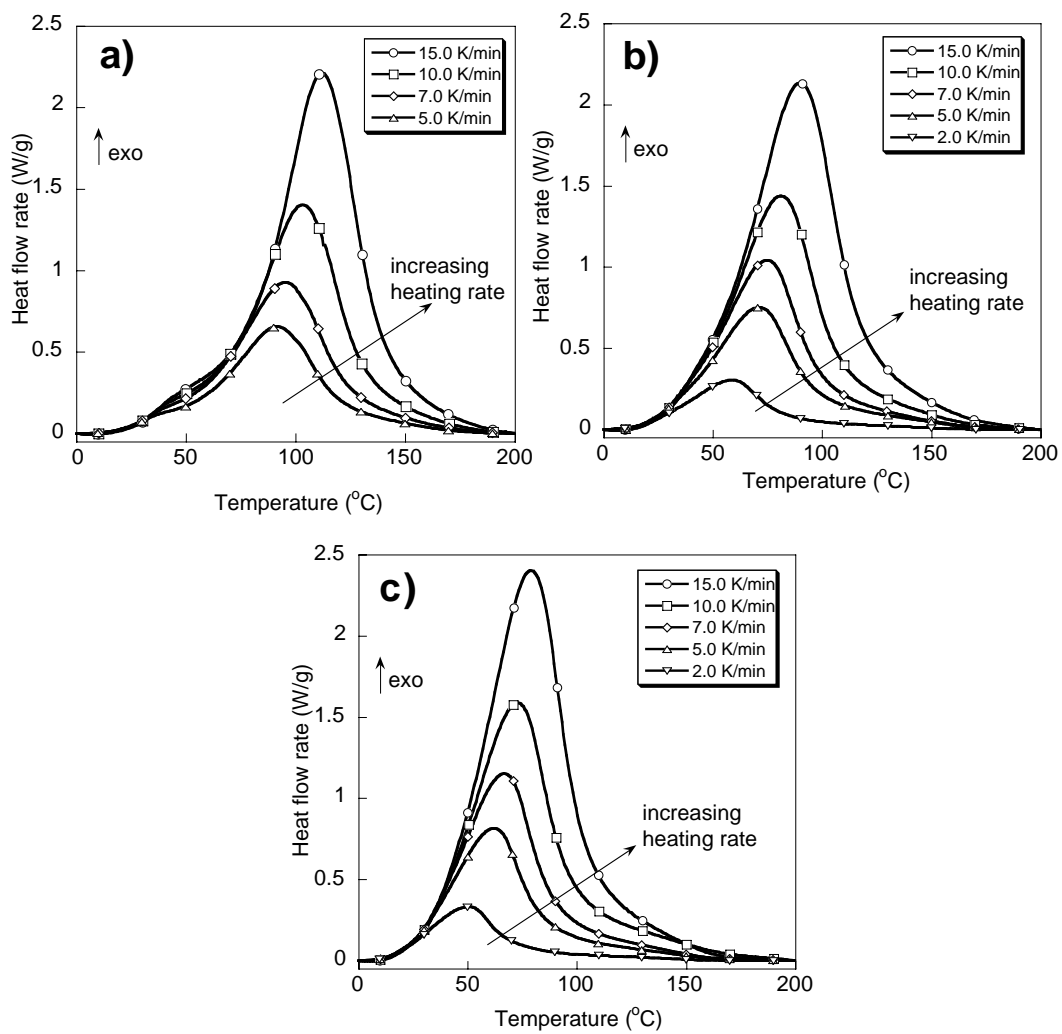(Note: 1:3750 catalyst concentration)

Figure 3. DSC curves for (a) low concentration, (b) medium concentration, and (c) high concentration, DCPD and Grubbs' catalyst samples.
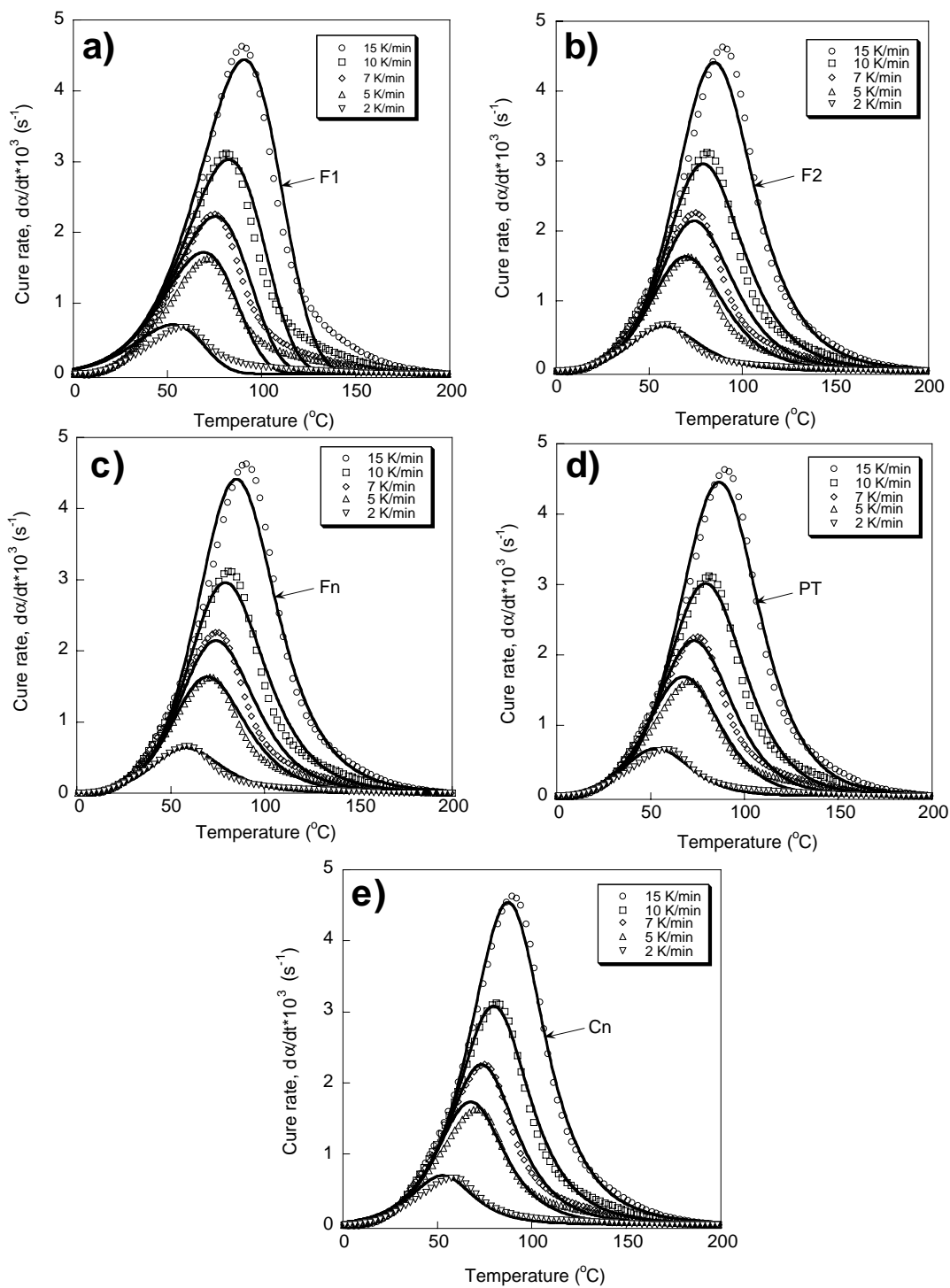
Figure 4. Model fits of DSC data for the medium catalyst concentration. (a) 1st order (F1), (b) 2nd order (F2), (c) nth order (Fn), (d) expanded Prout-Tompkins (PT), (e) nth order with autocatalysis (Cn).
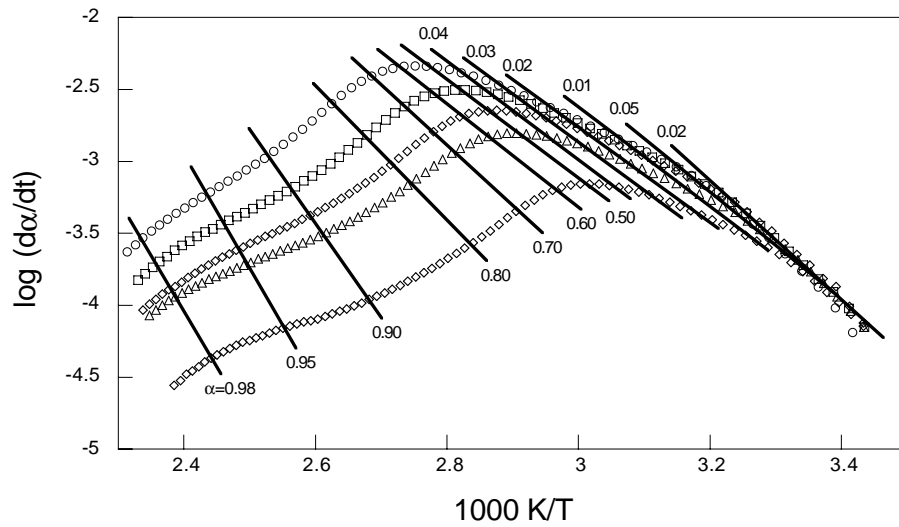
Figure 5. Friedman plot for medium catalyst concentration case.
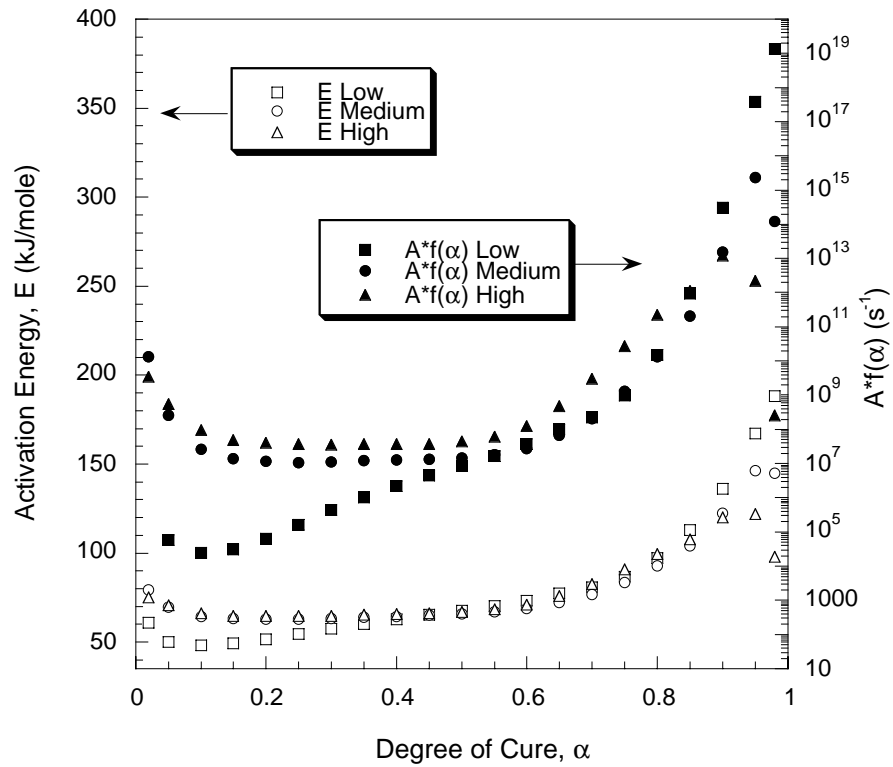
Figure 6. Model-free results for the activation energy and the product $A*f(\alpha)$ vs. degree of cure for all three catalyst concentration cases.
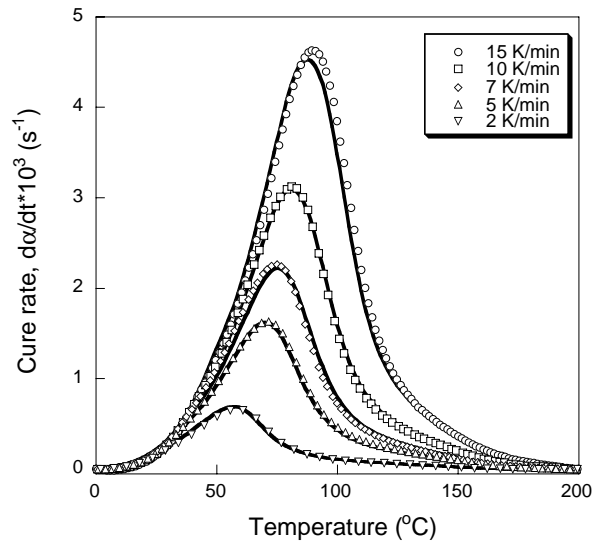
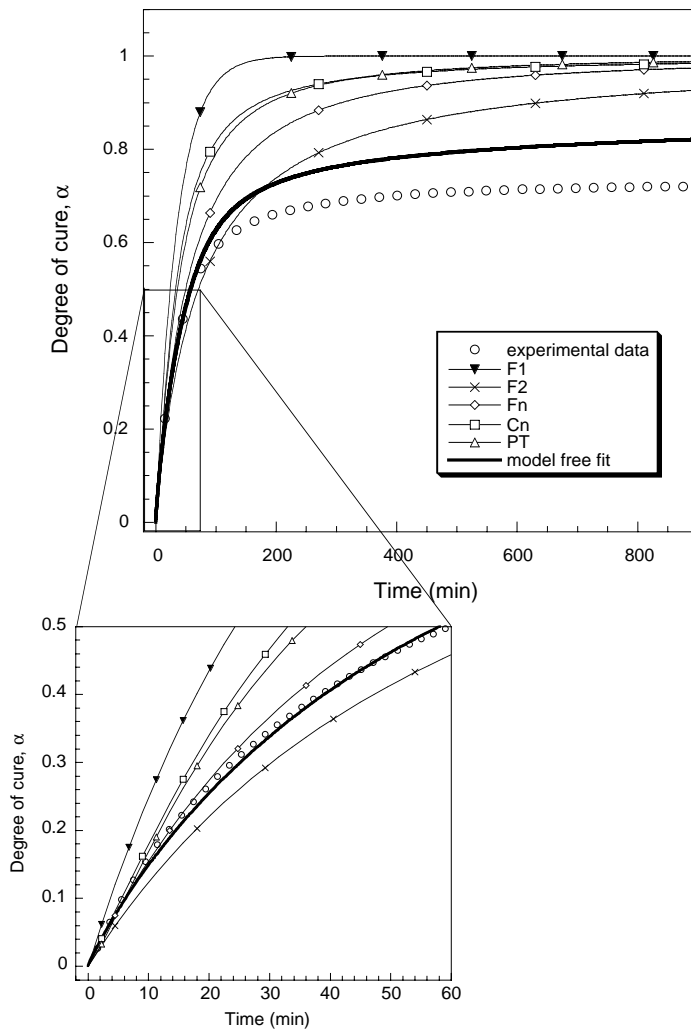Figure 7. Model-free prediction and experimental results for medium catalyst concentration case.

Figure 8. Model predictions for isothermal curing at 30°C for the medium catalyst concentration case overlaid with a 900 min isothermal cure experiment.
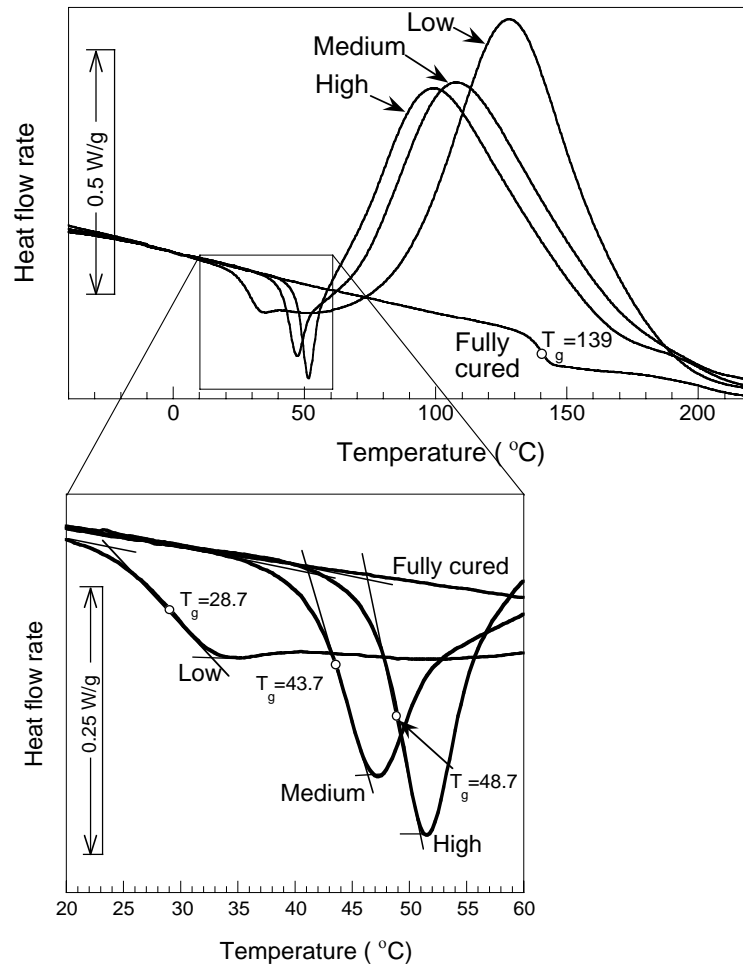
Figure 9. Dynamic scans (15°C/min) of fully cured control sample and samples just after the 30°C, 900 min isothermal runs for low, medium, and high concentrations.
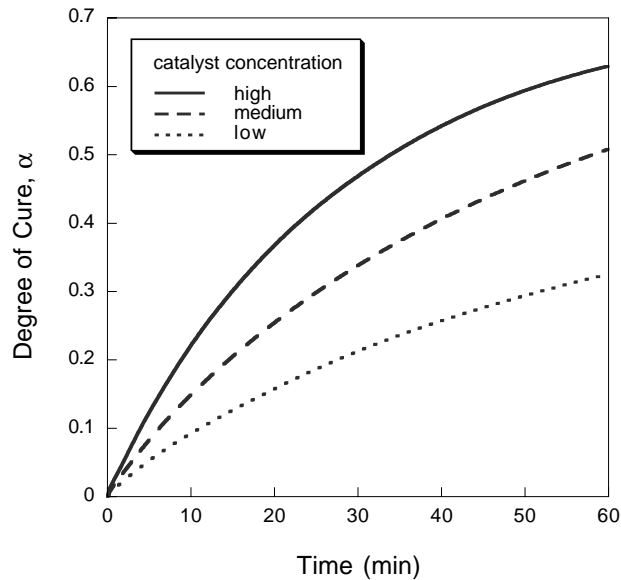

Figure 10. Predictions for isothermal curing at 30°C based on model-free isoconversional method for low, medium, and high catalyst concentrations.